Double-layer Chessboard AMC Surface for RCS Reduction in an Ultra-wide Band

Xueyan Song [1], Lei Chen [2], Zehong Yan [2], Yunqi Zhang [1], and Haitao Song [3]

[1] School of Electronic Engineering
Xi'an University of Posts & Telecommunications, Xi'an, 710121, China
xysong6597@126.com, johnny_5@126.com

[2] National Key Laboratory of Antennas and Microwave Technology
Xidian University, Xi'an, 710071, China
leichen@mail.xidian.edu.cn, zhyan@mail.xidian.edu.cn

[3] Complex Systems Research Center, Shanxi University
Taiyuan, Shanxi, 030006, China
htsong@sxu.edu.cn

Abstract ─ A novel chessboard surface is proposed for ultra-wideband radar cross section (RCS) reduction. The designed artificial magnetic conductor (AMC) surface is arranged by two different double-layer AMC unit cells, bringing in destructive reflection phase difference (180°±37°) in an ultra-wide band ranging from 5.8 to 16.1 GHz (94.06%). Each double-layer unit cell consists of a substrate layer loaded with metal patches and a PEC layer, in between of which is a 2-mm-thick air gap, which results in smooth phase curves of the two AMC units. One of the metal patches is composed of an octagonal ring and a Union Jack cross, and the other one is a Jerusalem cross. With chessboard arrangement by the two units, the RCS of the proposed surface can be reduced by more than 10 dB over a 90.22% frequency range (6.23-16.47 GHz) for both x and y polarizations. And the 20-dB RCS reduction frequency band ranges from 12.3 GHz to 15.9 GHz (25.5%). Then, the proposed AMC surface is fabricated and measured, and the measured 10-dB RCS reduction frequency band ranges from 6.66 to 16.42 GHz (84.58%) for x polarization and from 6.65 to 16.5 GHz (85.1%) for y polarization, which verifies that the presented AMC configuration may achieve potential applications on low-RCS platforms in an ultra-wide band.

Index Terms ─ Artificial Magnetic Conductor (AMC), Radar Cross Section (RCS) reduction, ultra-wideband.

I. INTRODUCTION

With the development of new electromagnetic metamaterials, the study on AMC has gradually been a hot research in fields of microwave. Thanks to their unique in-phase reflection properties, planar AMCs have been found many applications, such as suppression of surface waves in antenna designs [1], reducing the mutual coupling of units in antenna array designs [2], being utilized as artificial ground planes to achieve low-profile and gain-enhanced antennas [3], and reducing the RCS of platforms to achieve stealth in military fields [4]. Among them, contributing to solving the problems on thickness and bandwidth of traditional materials, such as Salisbury screen [5], metamaterial absorbers [6], etc., the application of AMC surfaces in RCS reduction [7-15] has recently been paid more and more attention. Radar cross section (RCS) is integral to the development of radar stealth technology [15]. RCS reduction (RCSR) means reducing the electromagnetic backscattered waves, which is essential in stealth technology [13]. An EBG checkerboard surface can result in a redirecting of the scattered fields [16], which bringing about a decrease in RCS.

In 2007, a planar structure combined of AMC and perfect electric conductor (PEC) unit cells in a chessboard is designed for RCS reduction applications [4]. Based on the opposite reflection phase of AMC and PEC, the reflections in normal direction cancel out, thus reducing the RCS. However, the bandwidth of the chessboard is limited by the narrow in-phase reflection (±37°) frequency band of AMC. In order to enhance the RCS reduction bandwidth, PEC can be substituted by another AMC, and surfaces consisting of AMC structures [7-12] have gradually been presented. In [7], two different types of AMC unit cells are periodically designed to form a planar surface, which achieve a +143° ~ +217° phase difference in the band from 13.25 to 24.2 GHz for boresight RCS reduction. After that, composite surfaces, consisting of two kinds of AMC

Submitted On: January 11, 2020
Accepted On: May 21, 2020

units, are proposed in [8] and [9], which achieve a nearly 10 dB RCS reduction over a 32% and 40% bandwidth, respectively. Moreover, combined by two Jerusalem Crosses with different sizes, a planar chessboard structure is proposed [10] and obtained about 42% bandwidth for 10 dB RCS reduction. With the same method, a miniaturized AMC reflecting screen combined by square unit cells with different sizes is recently designed [11] and the RCS is reduced in the band from 13.4 GHz to 26.9 GHz (67%).

Nevertheless, the bandwidth of RCS reduction in the previous researches needs to be furtherly widened to meet the requirements of objects for stealth in an ultra-wide band. For the purpose of a further increase in the bandwidth, double-layer AMC structure is proposed in [12]. By using an air layer, a novel double-layer chessboard surface is presented, and 73% bandwidth for 10 dB RCS reduction is obtained. The top layer is formed by substrate and substrate printed with a circular patch, and the bottom layer is PEC ground. Loading with the air gap, two smooth phase curves of the AMC units can be obtained, resulting in a wide phase difference bandwidth. Then, double-layer and multi-layer AMC surfaces are proposed in succession [13-15]. In [13], a three-layer chessboard-like AMC structure formed by two crossed ellipses with different sizes is proposed and obtain wide 10 dB RCS-reduction bandwidth from 8.11 to 23.32 GHz. In addition, a chessboard AMC surface based on the quasi-fractal structure is proposed in [14], and realizes a 10-dB RCS reduction band ranging from 5.4 GHz to 14.2 GHz. In 2019, a double-layer checkerboard AMC structure with two kinds of AMC elements is designed [15] and observe 10 dB RCS reduction in the band from 3.77 to 10.14 GHz.

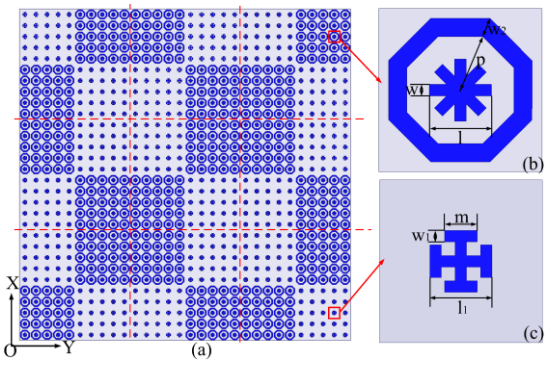

Fig. 1. Top view of the proposed AMC surface and unit cells. (a) Chessboard AMC surface, (b) AMC unit cell$_1$, and (c) AMC unit cell$_2$. Dimensions (unit: mm): l=3.8, p=3.55, w=0.7, w_2=1.2, l_1=4.0, w_1=0.8, m=2.

In this paper, a novel double-layer AMC configuration is designed here to further improve the bandwidth and increase the RCS reduction value. On the top layer, the patch array is composed of two kinds of AMC patches instead of combination by AMCs and PECs. One kind of AMC patches is an octagonal ring with a Union Jack cross, and the other one is a Jerusalem Cross. The simulated results show that the frequency band of reflection phase difference (180°±37°) between the two AMC unit cells ranges from 5.8 to 16.1 GHz (94.06%). And a 90.22% fractional bandwidth (6.23-16.47 GHz) for both x and y polarizations is obtained for 10 dB RCS reduction. In addition, a 20-dB RCS reduction frequency band ranging from 12.3 GHz to 15.9 GHz (25.5%) can be obtained for both x and y polarizations. The measured RCS reduction frequency bands are 6.66-16.42 GHz for x polarization and 6.65-16.5 GHz for y polarization, which agree well with the simulated ones.

II. AMC DESIGN AND SIMULATED RESULTS

A. Design principle of broadband AMC surface

From reference [16], the expression of the AMC surface for RCS reduction can be obtained from the following formula [17-18]:

$$\text{RCS reduction} = 10\log_{10}\left|\frac{A_1 e^{j\varphi_1} + A_2 e^{j\varphi_2}}{2}\right|^2, \qquad (1)$$

where, A_1 and A_2 is the reflection magnitude of AMC$_1$ and AMC$_2$, respectively; φ_1 and φ_2 are their reflection phases. Generally, a 10 dB RCS reduction in boresight direction compared to PEC sheet with the equal size is set as a criterion [19]. Therefore, from formula (1), the effective reflection phase difference of the AMC surface is

$$143° \le \left|\varphi_2 - \varphi_1\right| \le 217°. \qquad (2)$$

For this reason, 180°±37° is considered as the effective phase difference for analysis in follows.

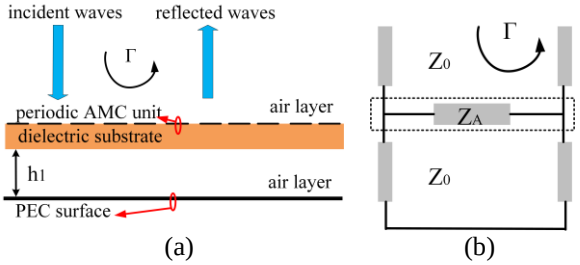

Fig. 2. (a) Double-layer AMC structure, and (b) its equivalent transmission line model.

Therefore, to achieve ultra-wideband 10 dB RCS reduction, two AMC units, which can generate 180°±37°

phase difference in an ultra-wide band, need to be designed firstly. Because of the excellent performances, double-layer AMC structure is finally chosen for wideband 10-dB RCS reduction. Based on the research in reference [15], the double-layer AMC structure and its equivalent transmission line model can be depicted as Fig. 2. Z_A and Z_0 refer to the equivalent impedance of the periodic structure and the intrinsic impedance of air layer, respectively. h1 is the height between the top layer and the PEC layer. Z_A can be approximately expressed as $Z_A \approx jX_A$. The impedances can be replaced by the admittances. Therefore, $Y_A = 1/Z_A \approx jB_A$, and $Y_0 = 1/Z_0$.

According to [15], the reflection coefficient and phase of an AMC can be expressed as:

$$\Gamma = \frac{Y_0(j\sin(\beta_0 h_1) - \cos(\beta_0 h_1)) - jY_A \sin(\beta_0 h_1)}{Y_0(j\sin(\beta_0 h_1) + \cos(\beta_0 h_1)) + jY_A \sin(\beta_0 h_1)}, \quad (3)$$

$$\varphi = 2\arctan\left(\frac{Y_0 \sin(\beta_0 h_1)}{-Y_0 \cos(\beta_0 h_1) + B_A \sin(\beta_0 h_1)}\right), \quad (4)$$

where, $\beta_0 = 2\pi f / c$ refers to the phase constant in vacuum, and f is the operation frequency. Moreover, for total cancellation, the susceptance of the AMC periodic structure can be calculated as:

$$B_A = Y_0 \cot(\beta_0 h_1) + Y_0 \tan(sf + a), \quad (5)$$

Where s is related to rate of reflection phase and a is related to initial value of reflection phase, and the unit of frequency (f) is gigahertz. And the independence of periodic structure for AMC unit1 and unit2 can be written as:

$$Z_{A1} = \frac{1}{jB_{A1}} = \frac{-jZ_0}{\cot(\beta_0 h_1) + \tan(sf + a)}, \quad (6)$$

$$Z_{A2} = \frac{-jZ_0}{\cot(\beta_0 h_1) - \cot(sf + a)}. \quad (7)$$

From (6) and (7), AMC unit1 can be approximately parallel resonance when AMC unit2 is series resonance. Or, AMC unit1 can be approximately series resonance when AMC unit2 is parallel resonance.

B. Design and analysis of AMC surface

After sufficiently analyzing the frequency behaviors of various AMC units, the two unit cells in Fig. 1 are selected to constitute the proposed AMC surface. Using a Floquet port and Master/Slave boundaries, a full-wave analysis is carried out by ANSYS HFSS. And Figs. 3 (a) and (b) demonstrate the simulated configuration of the two units, both of which are double-layer structures with dimensions of 10×10 mm^2. The top layer is a metal patch etched on a 2-mm-thickness F4BM-2 dielectric substrate (ε_r=2.2, tanδ=0.0007), and the bottom layer is a PEC sheet. Between two layers is an air gap with height of h1, which contributes to smooth phase curves of the two AMC units. An octagonal ring with a Union Jack cross patch constitutes AMC unit cell1 and a Jerusalem Cross patch comprises AMC unit cell2. Figures 3 (c) and (d) depict the equivalent circuit models for the two AMC units [20]. It can be seen from the equivalent circuit models that the AMC unit cell1 can is a series resonance circuit and the AMC unit cell2 is a parallel resonance circuit, which accords with the cancelation conditions mentioned above.

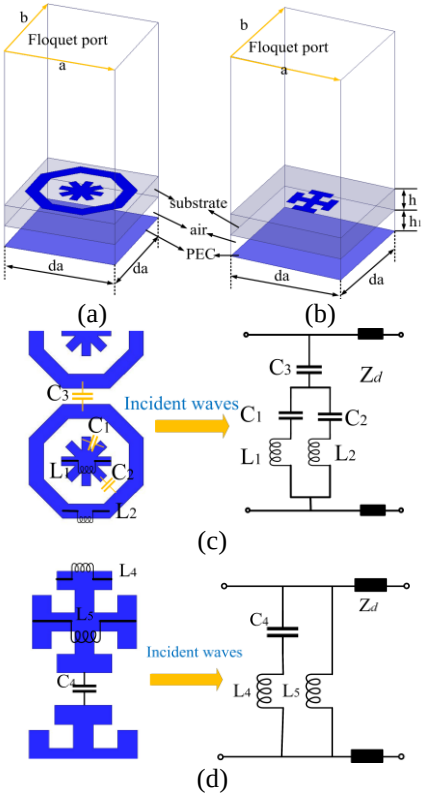

Fig. 3. Simulation model and equivalent circuit models of the proposed AMC unit cells. (a) AMC unit cell$_1$ and (b) AMC unit cell$_2$. h=2mm, h$_1$=2mm, da=10mm. (c) Equivalent circuit model for AMC unit cell$_1$, and (d) equivalent circuit model for AMC unit cell$_2$.

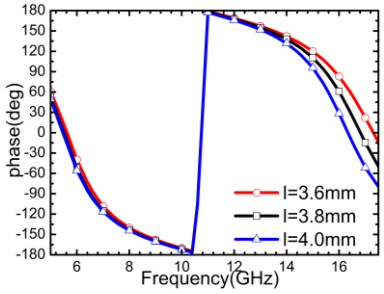

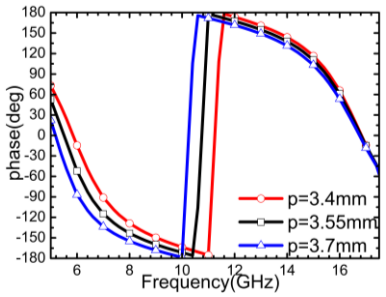

(b)

Fig. 4. Impact of parameters (a) l and (b) p on the reflection phase of AMC unit cell$_1$.

Figure 1 depicts dimensions of the two designed unit cells. Of all the parameters, parameters l and p have a great impact on the reflection phase property of the two AMC unit cells, which can be seen in Figs. 4 (a-b). The values of l and p determine the two resonances of unit cell1 in the high and low frequency band, respectively. When l increases from 3.6mm to 4mm, the equivalent inductance L1 and capacitance C2 in Fig. 3 (c) increase, which leads to a decrease in the resonances in the low frequency band, as can be seen in Fig. 4 (a). Similarly, with an increase in p, the circumference of the square loop increases, bringing about the increase in the inductance L2 of the octagonal loop the mutual coupling capacitance C3. Therefore, the resonant frequency in low band decreases, which corresponds to the simulated results in Fig. 4 (b). To obtain a wide phase difference band, the values of l and p are finally decided to be 3.8mm and 3.55mm, respectively.

Figure 5 demonstrates the simulated reflection phase and difference of two AMC unit cells. Consisting of an octagonal ring and a Union Jack cross patch, AMC unit cell1 can generate two resonances in the low and high frequency band, respectively, as depicted in Fig. 4 (a), thus arising two different 0° phase reflection frequencies (5.5 GHz and 17.8 GHz) and a 180° phase reflection at 10.8 GHz. Whereas, AMC unit cell2 exhibits 0° phase reflection value at 11.6 GHz, which is close to the 180° phase reflection frequency of AMC unit cell1, thus giving birth to an ultra-wide reflection phase difference (180°±37°) band from 5.8 to 16.1 GHz for normal incidence. Hence, an ultra-wideband 10 dB RCS reduction with a percentage bandwidth of 94.06% can be expected.

In addition, the phase differences under different incident angles are also simulated and depicted in Fig. 6. It can be obtained that the bandwidths of phase difference keep stable when the incident angle is lower than 15°, and when the incident angle is increased to 30° and 45° the phase difference band changes to double bands. And with the increase in incident angle, the phase difference bandwidth decreases.

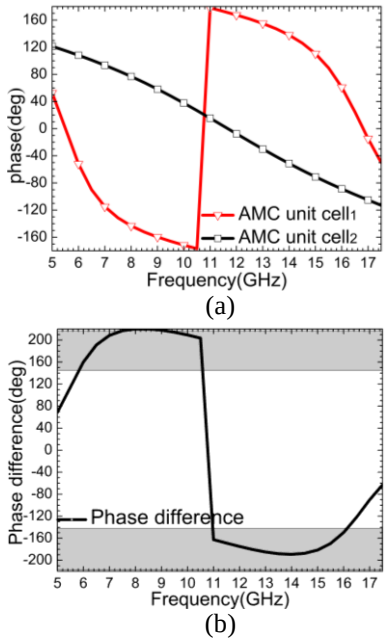

Fig. 5. Simulated reflection phase and difference of AMC unit cells. (a) Reflection phase and (b) reflection phase difference.

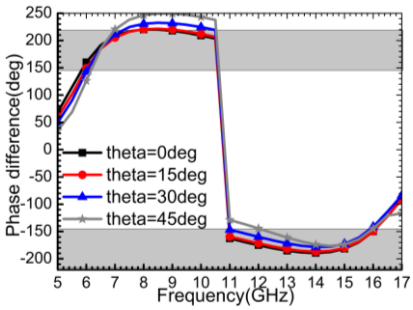

Fig. 6. Reflection phase difference for different incident angles.

For the sake of low RCS property in an ultra-wide band, the surface is combined by 3×3 chessboard's cell arrays, as demonstrated in Fig. 1 (a). Each chessboard cell array is made up of 10×10 unit cells, and arranged by 5×5 AMC unit cell1 and 5×5 AMC unit cell2. Dimensions of the proposed AMC surface are 300×300×4 mm^3. To calculate the RCS reduction bandwidth of the designed chessboard surface, the monostatic RCS of the AMC surface and PEC surface with equal size for normal incidence is simulated. As depicted in Fig. 4, parameters l and p have a great influence on the reflection phase property. To investigate the effect of those two parameters on the RCS reduction of AMC surface, the RCS reduction of AMC surface with

different l or p is simulated, and Fig. 7 shows the simulated results. It can be obtain from Fig. 7 that the change in parameter l has an influence on the 10-dB RCS reduction bandwidth and the largest reduction value in the high frequency band, and parameter p affects the largest reduction value in low frequency band and the RCS reduction bandwidth, which corresponds to the results in Fig. 4. In compromising of the value and bandwidth of RCS reduction, l and p is finally selected as 3.8mm and 3.55mm, respectively.

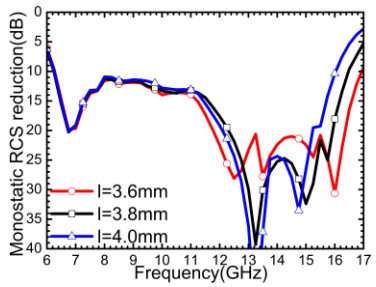

Fig. 7. Impact of parameters (a) l and (b) p on the simulated monostatic RCS reduction.

Then, Fig. 8 depicts the final simulated monostatic RCS and RCS reduction of proposed AMC surface under normal incidence for both x and y polarizations. From the simulated results, an ultra-wide 10-dB RCS reduction frequency band ranging from 6.23 GHz to 16.47 GHz (90.22%) is achieved. And the maximum RCS reduction, which is more than 35 dB, is obtained at 13.4 GHz. Compared with references [12-15], the AMC surface can achieve larger RCS reduction value and wider 20-dB RCS reduction frequency band ranging from 12.3 GHz to 15.9 GHz (25.5%). Furthermore, Fig. 9 demonstrates the normalized 2-D bistatic RCS of PEC sheet and the proposed AMC configuration under different incidences for both x and y polarizations at 13.4 GHz. Compared with the bistatic RCS of the PEC surface in Fig. 9, the proposed AMC surface can achieve low RCS in boresight direction and reflects the scattering energy in other directions.

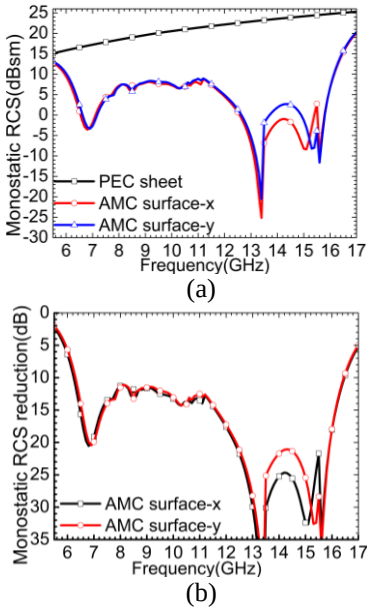

Fig. 8. Simulated monostatic RCS and RCS reduction of proposed chessboard AMC surface under normal incidence for both *x* and *y* polarizations. (a) Monostatic RCS and (b) RCS reduction.

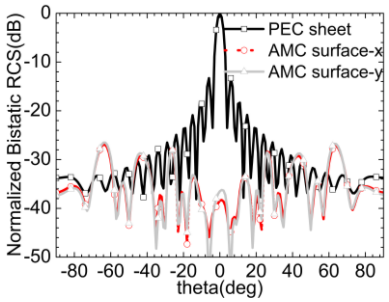

Fig. 9. Simulated normalized 2-D bistatic RCS pattern of proposed AMC surface and PEC sheet under different incidences for both *x* and *y* polarizations at 13.4GHz.

In order to investigate the change of RCS reduction with different incident angles, Fig. 10 demonstrates the simulated bistatic RCS reduction under different incident angles for both x and y polarizations. From the simulated results, it can be obtained that the values of RCS reduction decrease with the increase in incident angle, which is corresponding to the simulated phase differences under different incident angles. And the changes in RCS reduction values are related with the instability of the AMC structure with incident angles.

In view of the good RCS reduction property of the proposed AMC surface, the proposed AMC unit cells can be arranged periodically around the antenna on the

same plane when an antenna need to be obtained low RCS performance, just as the structures in references [9] and [11].

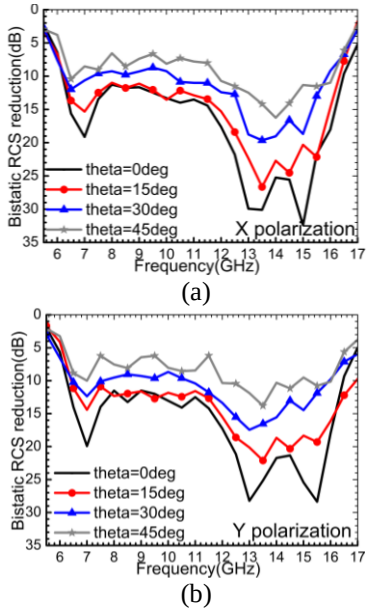

Fig. 10. Simulated bistatic RCS reduction under different incident angles for (a) x and (b) y polarizations.

III. FABRICATION AND MEASURED RESULTS

To verify the simulated results, the proposed chessboard surface is fabricated, as shown in Fig. 11. 30×30 unit patches are etched on a 2-mm-thickness F4BM-2 dielectric substrate. Separated by a 2-mm-thickness air gap, a PEC sheet (a replacement by a thin aluminum sheet) is installed beneath the substrate layer. The total dimensions of the proposed structure are 300×300×4 mm^3. To show the ability for RCS reduction, the RCS values of the proposed AMC surface are normalized by the PEC sheet with the identical physical dimensions. The measured and simulated monostatic RCS of the proposed AMC surface and PEC sheet is depicted in Fig. 12 (a). And Fig. 12 (b) illustrates the measured and simulated RCS reduction of the designed chessboard configuration.

From the measured results depicted in Fig. 12, the RCS of the designed AMC surface can be reduced by more than 10 dB in the band ranging from 6.66 to 16.42 GHz (84.58%) for x polarization and from 6.65 to 16.5 GHz (85.1%) for y polarization under normal incident waves. Due to the fabricated and measured errors and the error in the height between the top and the bottom layers, there is a little frequency shifting in the measured RCS reduction frequency band compared with the simulated results and the measured values of RCS reduction are a little higher than the simulated ones.

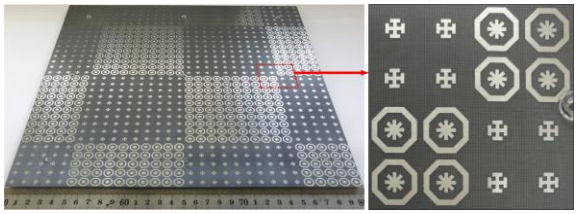

Fig. 11. Photograph of fabricated chessboard surface.

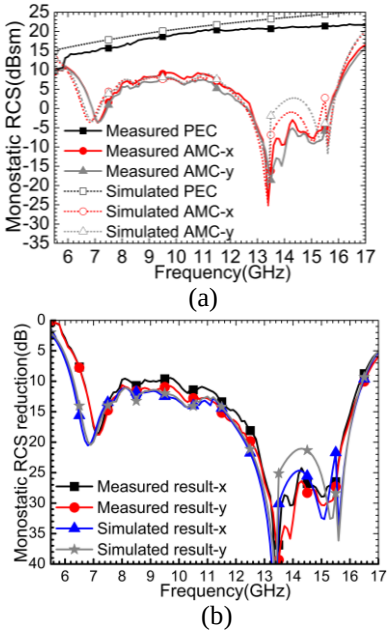

Fig. 12. Measured and simulated monostatic RCS and RCS reduction of proposed chessboard AMC surface under normal incidence for both *x* and *y* polarizations. (a) monostatic RCS and (b) RCS reduction.

IV. CONCLUSION

In this letter, a novel double-layer chessboard AMC surface is presented for RCS reduction in an ultra-broad band. In the expectation of a wider RCS reduction frequency band, the proposed chessboard configuration is formed by two different double-layer AMC unit cells. The patch printed on the substrate of one unit is an octagonal ring with a Union Jack cross, and that of the other one is a Jerusalem cross. With the two different unit cells, an ultra-broad reflection phase difference (180°±37°) band from 5.8 to 16.1 GHz can be obtained. Arranged by the two double-layer unit cells, the designed AMC surface achieves an ultra-wide frequency band ranging from 6.23 to 16.47 GHz (90.22%) for 10 dB RCS reduction under normal incidence for both x and y polarizations. In the band from 12.3 GHz to 15.9 GHz (25.5%), the RCS can be reduced for more than 20 dB. The measured results show that the fabricated prototype can achieve a 10-dB RCS reduction frequency band of 6.66-16.42 GHz for x

polarization and of 6.65-16.5 GHz for y polarization, which validates that the designed AMC surface can be utilized for ultra-wideband RCS reduction applications.

ACKNOWLEDGMENT

This work is supported by the National Natural Science Foundation of China (61671304 and 11601291) and the Scientific Research Program Funded by Shaanxi Provincial Education Department (18JK0701).

REFERENCES

[1] X. C. Wei, Y. F. Shu, J. B. Zhang, and D. Wang, "Applications of high impedance surfaces for surface wave elimination," *2016 URSI Asia-Pacific Radio Science Conference (URIS AP-RASC)*, Seoul, South Korea, pp. 1458-1461, 2016.

[2] L. Mouffok, L. Damaj, X. Begaud, A. C. Lepage, and H. Diez, "Mutual coupling reduction between dual polarized microstrip patch antennas using compact spiral artificial magnetic conductor," *Proceedings of the 5th European Conference on Antennas and Propagation (EUCAP)*, Rome, Italy, pp. 909-912, 2011.

[3] B. Zhang, P. Yao, and J. Duan, "Gain-enhanced antenna backed with the fractal artificial magnetic conductor," *IET Microwaves Antennas Propag*., vol. 12, pp. 1457-1460, 2018.

[4] M. Paquay, J. C. Iriarte, I. Ederra, R. Gonzalo, and P. Maagt, "Thin AMC structure for radar cross-section reduction," *IEEE Trans. Antennas Propag*., vol. 55, pp. 3630-3638, 2007.

[5] K. L. Ford and B. Chambers, "Tunable single layer phase modulated radar absorber," *2001 Eleventh International Conference on Antennas and Propagation*, Manchester, UK, pp. 588-592, 2001.

[6] Y. Ishii, T. Masaki, N. Michishita, H. Morishita, and H. Hada, "RCS reduction characteristics of thin wave absorbers composed of flat and curved metasurfaces," *2016 International Symposium on Antennas and Propagation (ISAP)*, Okinawa, Japan, pp. 192-193, 2016.

[7] Y. Zhang, R. Mittra, B. Z. Wang, and N. T. Huang, "AMCs for ultra-thin and broadband RAM design," *Electron. Lett*., vol. 45, pp. 484-485, 2009.

[8] Y. Fu, Y. Li, and N. Yuan, "Wideband composite ANC surfaces for RCS reduction," *Microwave Opt. Technol. Lett*., vol. 53, pp. 712-715, 2011.

[9] Y. J. Zheng, J. Gao, X. Y. Cao, Z. Yuan, and H. Yang, "Wideband RCS reduction of a microstrip antenna using artificial magnetic conductor structures," *IEEE Antennas Wireless Propag. Lett.*, vol. 14, pp. 1582-1585, 2015.

[10] J. C. I. Galarregui, A. T. Pereda, J. L. M. Falcón, I. Ederra, R. Gonzalo, and P. Maagt, "Broadband radar cross-section reduction using AMC technology," *IEEE Trans. Antennas Propag*., vol. 61, pp. 6136-6143, 2013.

[11] Y. Pei, B. Zhang, and J. Duan, "A broadband artificial magnetic conductor reflecting screen and application in microstrip antenna for radar cross-section reduction," *IEEE Antennas Wireless Propag. Lett*., vol. 17, pp. 405-409, 2018.

[12] M. Mighani and G. Dadashzadeh, "Broadband RCS reduction using a novel double layer chessboard AMC surface," *Electron. Lett*., vol. 52, pp. 1253-1255, 2016.

[13] R. Zaker and A. Sadeghzadeh, "Wideband radar cross section reduction using a novel design of artificial magnetic conductor structure with a triple-layer chessboard configuration," *International Journal of RF and Microwave Computer‐Aided Engineering*, e21545, 2018.

[14] J. Xue, W. Jiang, and S. Gong, "Chessboard AMC surface based on quasi-fractal structure for wideband RCS reduction," *IEEE Antennas and Wireless Propagation Letters*, vol. 17.2, pp. 201-204, 2018.

[15] D. Sang, Q. Chen, L. Ding, M. Guo, and Y. Fu, "Design of checkerboard AMC structure for wideband RCS reduction," *IEEE Transactions on Antennas and Propagation*, pp. 2604-2612, 2019.

[16] W. Chen, C. A. Balanis, and C. R. Birtcher, "Checkerboard EBG surfaces for wideband radar cross section reduction," *IEEE Trans. Antennas Propag*., vol. 63, pp. 2636-2645, 2015.

[17] A. Y. Modi, C. A. Balanis, C. R. Birtcher, and H. N. Shaman, "Novel design of ultrabroadband radar cross section reduction surfaces using artificial magnetic conductors," *IEEE Trans. Antennas Propag*., vol. 65, pp. 5406-5417, 2017.

[18] W. Q. Chen, C. A. Balanis, C. R. Birtcher, and A. Y. Modi, "Cylindrically curved checkerboard surfaces for radar cross section reduction," *IEEE Antennas Wireless Propag. Lett*., vol. 17, pp. 343-346, 2018.

[19] Y. Zhao, X. Y. Cao, J. Gao, X. Yao, and X. Liu, "A low-RCS and high-gain slot antenna using broadband metasurface," *IEEE Antennas Wireless Propag*., vol. 15, pp. 290-293, 2016.

[20] D. Singh, A. Kumar, S. Meena, and V. Agarwala, "Analysis of frequency selective surfaces for radar absorbing materials," *Progress in Electromagnetics Research B*, vol. 38, pp. 297-314, Feb. 2012.

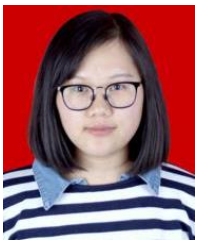

Xueyan Song was born in Henan Province, China, 1989. She received the B.E. degree in Electronic and Information Engineering from Xidian University, Xi'an, China, in 2012. She received the Ph.D. degree in Electromagnetic Fields and Microwave Technology from Xidian University, Xi'an, China, in 2018.

She joined the School of Electronic Engineering, Xi'an University of Posts and Telecommunications in 2018. Her research interests include artificial magnetic conductors, low RCS antennas, low-profile antennas, frequency selective surfaces, and reflector antennas.

Lei Chen was born in Shaanxi Province, China, 1982. She received the Ph.D. degrees in Electromagnetic Fields and Microwave Technology from Xidian University, Xi'an, China, in 2010.

She is an Associate Professor at Xidian University. Her research interests include retrodirective array, reflectarray and smart antenna.

Zehong Yan was born in Hubei Province, China, 1964. He received the B.E. degree in Antenna and Microwave from Xidian University, Xi'an, China, in 1984. He received the Ph.D. degree in Electromagnetic Fields and Microwave Technology from Northwestern Polytechnical University, Xi'an, China, in 1996.

He joined the School of Electronic Engineering, Xidian University in 1987 and was promoted to Associate Professor and Professor in 1996 and 2000, respectively, where he is currently a Doctoral Supervisor with the School of Electronic Engineering. His research interests include communication antennas, satellite tracking antennas, and microwave devices.

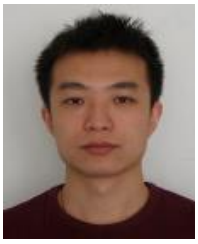

Yun-Qi Zhang was born in BaoTou, Inner Mongolia, China. He received the Ph.D. degree from Xidian University, Xi'an, China in 2015. He is currently working in the Xi'an University of Posts & Telecommunications. From 2017 he joined the school of Physics and Optoelectronic Engineering, Xidian University, as a Post Doctor. His research interests include GPS antenna, CP antenna, omnidirectional antenna and antenna array designs.

Haitao Song was born in Henan Province, China, 1986. He received the Ph.D. degree in Mathematics from Harbin Institute of Technology, Harbin, China, in 2014. He was a Postdoctoral Fellowship in York University, Toronto, Canada, from 2016 to 2018.

He is and Associate Professor at Shanxi University. His research interests include functional differential equations, dynamical system and theirs' applications.